ACS Macro Letters

Letter

pubs.acs.org/macroletters

Polymersomes from Amphiphilic Glycopolymers Containing Polymeric Liquid Crystal Grafts

Khalid Ferji,[†,‡,§] Cécile Nouvel,[†,‡] Jérôme Babin,[†,‡] Min-Hui Li,[∥] Cédric Gaillard,[⊥] Erwan Nicol,[§] Christophe Chassenieux,[§] and Jean-Luc Six*[,†,‡]

[†]Université de Lorraine, Laboratoire de Chimie Physique Macromoléculaire LCPM, UMR 7375, Nancy F-54000, France

[‡]CNRS, Laboratoire de Chimie Physique Macromoléculaire LCPM, UMR 7375, Nancy F-54000, France

[§]LUNAM Université, Université du Maine, Institut des Molécules et Matériaux du Mans UMR-CNRS 6283, Avenue Olivier Messiaen, F-72085 Le Mans cedex, France

[∥]Institut de Recherche de Chimie Paris, UMR8247, CNRS - Chimie ParisTech (ENSCP), 11 rue Pierre et Marie Curie, F-75231 Paris, France

[⊥]INRA, UR 1268 Unité Biopolymères Interactions Assemblages, F-44300 Nantes, France

Supporting Information

ABSTRACT: For the first time, polymersomes were obtained by self-assembly in water of amphiphilic grafted glycopolymers based on dextran polysaccharidic backbone and polymeric liquid crystal grafts (poly(diethylene glycol cholesteryl ether acrylate), PDEGCholA). After measuring the properties of these glycopolymers in term of surfactancy, the influence of their structural parameters on their self-assemblies once dispersed in water was investigated by static and dynamic light scattering and by cryogenic transmission electron microscopy (cryo-TEM). Based on the results, a proper design of Dex-g^{N}-PDEGCholA^{F} leads to hollow vesicular structure formulation known as polymersome.

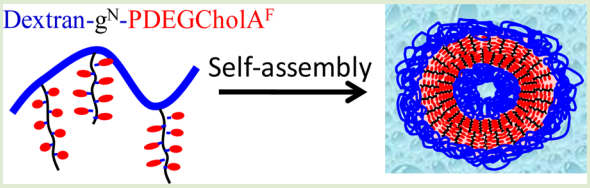

For many decades, researchers have been attempting to design model artificial membranes that can mimic the more complex biological ones by using phospholipids whose self-assembly in aqueous medium leads to vesicles commonly named liposomes.[1] More recently, polymeric counterparts of liposomes, so-called polymersomes, have been developed through the use of copolymers.[2] Usually, polymersomes are hollow spherical nano-objects composed of a hydrophobic compact bilayer membrane with hydrophilic inner and external surfaces. It was shown that this hydrophobic bilayer, thanks to its polymeric nature, enhances the mechanical stiffness and decreases the permeability to both solvent and solute than the ones of the liposomes.[3−5]

Such polymersomes were often produced by the self-assembly of amphiphilic block copolymers and found applications as drug delivery systems or nanoreactors.[6−9] Many reviews can be found dealing with the polymersome formulations from coil−coil diblock or triblock copolymers or with the experimental methods to investigate their vesicular morphology.[10,11] In order to improve the mechanical properties of the polymeric membrane, rod−coil diblock copolymers with block containing stiff moieties such as cholesterol or polypeptide were used. For instance, some mesogenic polymeric blocks have been considered in combination with various hydrophilic ones[12−22] and have been shown to result in stimuli-responsive polymersomes, which can be disrupted upon applying one external stimulus.[6,23,24] The design of smart polymersomes either responding to pH, temperature, redox, magnetic field, or light stimuli[6,11,25−27] has also been achieved thanks to the processing of new polymerization techniques and of chemical couplings. Biological polymers[7−9,28−31] like polypeptides, polynucleotides, or polysaccharides as well as biodegradable polymers such as polylactic acid (PLA) or poly(ε-caprolactone) (PCL) were also considered to produce polymersomes of interest for biological applications, especially when combined with biocompatible polyethylene glycol (PEG) block that leads to stealthy polymersomes.[32] However, the formation of polymersomes using other polymeric architectures than block copolymers such as graft copolymers has been reported to a far less extent. To the best of our knowledge, only four graft copolymers forming polymersomes have been investigated in the literature so far: poly(2-hydroxyethyl aspartamide)-*g*-oligo(lactic acid),[33] poly(β-amino ester)-*g*-(PEG/PLA),[34] chitooligosaccharide-*g*-PCL,[35] and poly(3-hydroxyoctanoate-*co*-3-hydroxyundecanoate)-*g*-PEG.[36]

The aim of the present study was to investigate the self-assembling propensity in solution and at the liquid/liquid interface of graft glycopolymers (called Dex-g^{N}-PDEGCholA^{F}) containing liquid-crystal (rod) grafts that were previously reported by us.[37] In these glycopolymers, dextran is used as the hydrophilic polysaccharidic backbone and poly(diethylene glycol cholesteryl ether acrylate) (PDEGCholA) as hydro-

Received: July 10, 2015
Accepted: September 15, 2015
Published: September 21, 2015

DOI: 10.1021/acsmacrolett.5b00471
ACS Macro Lett. 2015, 4, 1119−1122

Table 1. Characteristics of Dex-g^{N}-PDEGCholA^{F} and of Their Corresponding Nanostructures Formed in Aqueous Media

	copolymer characteristics				nanostructure characteristics				
entry	Dex-g^{N}-PADEGChol^{F}[a]	$\overline{M}_n$ of grafts[b] (g/mol)	$Đ$[c]	solvent (before dialysis)	R_h[d] (nm)	R_g[e] (nm)	R_g/R_h	polydispersity[f]	t[g] (nm)
C1	Dex-g^{24}-PADEGChol^{90}	5.800	1.2	DMSO					
				THF					
C2	Dex-g$^{6.6}$-PADEGChol^{73}	6.800	1.2	DMSO					
				THF					
C3	Dex-g^{5}-PADEGChol^{79}	12.600	1.2	DMSO	50	54	1.1	1.2	18.5 ± 1.0
				THF	68	63	0.9	1.1	20.0 ± 1.0[h]
C4	Dex-g$^{1.5}$-PADEGChol^{50}	11.000	1.3	DMSO	48	47	1.0	1.3	3.5 ± 0.5
				THF	62	67	1.1	1.2	6.5 ± 0.5

[a]N and F are the number of PDEGCholA grafts per 100 glucopyranosic units of dextran backbone and the weight fraction of PDEGCholA in amphiphilic glycopolymer, respectively. $\overline{M}_n$ and $Đ$ of dextran were estimated equal to 34.800 g mol^{-1} and 1.14, respectively.[37] [b]$\overline{M}_n$ of each PDEGCholA graft estimated from $([DEGCholA]_0/[Br]_0) \times M_0 \times conv$, where $[DEGCholA]_0$ and $[Br]_0$ are the initial molar concentrations of monomer and ATRP initiator groups carried by the macroinitiator (after steps i and ii, Scheme S1,[37]), respectively. M_0 is the molecular weight of the monomer unit of PDEGCholA (528 g mol^{-1}). [c]Dispersity of the corresponding acetylated copolymers (before step iv, Scheme S1[37]) measured by SEC in THF. [d]Hydrodynamic radius determined by dynamic light scattering. [e]Radius of gyration determined using Guinier plot. [f]See Supporting Information. [g]Membrane thickness of vesicles determined by fitting the Rayleigh ratio of the suspensions using eq S4. [h]Membrane thickness was estimated equal to 25 nm from Figure 2a.

phobic polymeric grafts. Various Dex-g^{N}-PDEGCholA^{F} were synthesized using a "grafting from" four-step strategy described in Scheme S1.[37] N and F, which are, respectively, the number of PDEGCholA grafts per 100 glucopyranosic units of dextran backbone and the weight fraction of PDEGCholA in glycopolymer, have been varied to some extent (Table 1).[37]

In bulk, PDEGCholA grafts appeared to exhibit both single glass transition and liquid crystal to isotropic transition temperatures. Between these two transition regimes, the bulk displayed at the microscopic scale typical smooth fan-shape birefringent textures, which indicated a smectic A phase, further confirmed by X-ray scattering measurements.[37] By comparing the lamellar period to the DEGCholA monomer length, we established that an interdigitated smecticA phase (SmA_d) was formed. This peculiar mesomorphism of the grafts was preserved once they were grafted onto a dextran backbone.[37]

In the present paper, we will focus more on the properties displayed by these graft glycopolymers when dispersed in solution. First, we will establish that these graft copolymers exhibit interfacial activities. Then, we will focus on the influence of the chemical structure of these copolymers onto the characteristics of their self-assemblies in water. Finally, we will show that these self-assemblies are actually of polymersome type.

Interfacial properties of Dex-g^{N}-PDEGCholA^{F} glycopolymers. In order to estimate the propensity of such glycopolymers to stabilize interfaces, we have dissolved two of them (entries C3 and C4, Table 1) in toluene (concentration lower than 0.2 g L^{-1}). After waiting 12 h at room temperature, in order to reach thermodynamic equilibrium, the interfacial properties of each Dex-g^{N}-PDEGCholA^{F} were evaluated by steady state interfacial tension (γ) measurements at the toluene/water interface as a function of copolymer concentration. As shown in Figure S1, the interfacial tension of a pure toluene/water interface was equal to 28.8 mN m^{-1}. By adding the graft glycopolymer, γ steadily decreased until A_1 = 1.5 mg L^{-1} (case of Dex-g^{5}-PDEGCholA^{79}, entry C3, Table 1) or A_2 = 6.2 mg L^{-1} (case of Dex-g$^{1.5}$-PDEGCholA^{50}, entry C4, Table 1), where the decrease of γ was much more pronounced. As shown in Table 1, each studied glycopolymer exhibits $Đ \neq 1$, meaning they are heterogeneous in composition (number and length of grafts). Nevertheless, as the length of the PDEGCholA grafts is roughly the same for both copolymers, the number of grafts onto the dextran backbone could account for such a difference: decreasing this number increased the concentration at which γ decreased. Above A_1 or A_2, γ decreased more steeply with increasing polymer concentration. Unfortunately, when the Dex-g^{N}-PDEGCholA^{F} concentration was too high, we observed a white polymeric layer located at the interface that prevented reliable measurements of γ. Consequently, the concentration range where the investigations were possible is rather limited. Nevertheless, the decrease of γ upon increasing polymer concentration can be related to their ability to stabilize the toluene/water interface as molecular surfactant does. Furthermore, the grafted nature of these amphiphilic copolymers and mesomorphic transitions of grafts could account for the broadening of the transition, which is far from being critical by opposition to what is encountered with molecular surfactants or even amphiphilic diblock copolymers.

Self-assembly of Dex-g^{N}-PDEGCholA^{F} glycopolymers. The ability for self-assembly of these graft glycopolymers was further investigated in water (Figure S2). First, Dex-g^{N}-PDEGCholA^{F} were dispersed either in THF at 25 °C or in DMSO at 100 °C, and then dialyzed against water (a selective solvent for dextran) during 2 days. Finally, the morphology of their self-assemblies was investigated by dynamic and static light scattering (DLS and SLS, respectively) and by cryogenic transmission electron microscopy (cryo-TEM). The characteristics of these nano-objects are summarized in Table 1. Nanostructures obtained with the copolymer Dex-g$^{1.5}$-PADEGChol^{50} (entry C4, Table 1) dissolved in DMSO or in THF are denominated C_4^{DMSO} or C_4^{THF}, respectively.

Depending on the number and the length of the grafts, two situations have been encountered. For copolymers containing a high number of short hydrophobic grafts ($\overline{M}_n$ of graft <7.000 g mol^{-1}, entries C1 and C2, Table 1), a precipitate was formed during dialysis, with whatever the organic solvent we used (THF or DMSO). By opposition, when copolymers containing a moderated number of long grafts ($\overline{M}_n$ of graft 11.500 g mol^{-1}, entries C3 and C4, Table 1) were considered, nano-objects were produced.

In these last cases, the dispersions are characterized by a single distribution of relaxation times in DLS over the whole scattering range investigated (from $\mathbf{q} = 4.6 \times 10^{-3}$ nm^{-1} to 2.55

DOI: 10.1021/acsmacrolett.5b00471
ACS Macro Lett. 2015, 4, 1119−1122

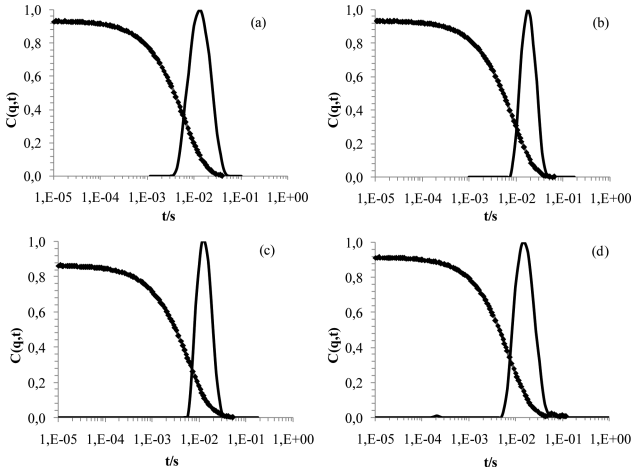

Figure 1. Autocorrelation functions $C(q,t)$ as a function of time and corresponding relative distribution of relaxation times recorded at a scattering wave vector $\mathbf{q}$ = 4.6 × 10^{-3} nm^{-1} (θ = 20°) for different nanostructures dispersed in water: (a) C_3^{DMSO}, (b) C_3^{THF}, (c) C_4^{DMSO}, (d) C_4^{THF}.

× 10^{-2} nm^{-1}), as shown in Figure 1 that displays typical examples of autocorrelation functions measured at the same scattering angle for each dispersion. The relaxation time derived from the autocorrelation functions displayed a q^2 dependence (Figure S3), which meant that diffusive motions of the scatterers were probed and which allowed us to estimate their hydrodynamic radius (R_h) using the Stokes−Einstein eq (eq S2). As shown in Table 1, R_h ranged between 47 and 68 nm, with a polydispersity close to 1 (see Supporting Information). In addition, the radius of gyration (R_g) for each dispersion was estimated by static light scattering measurements using the Guinier approximation. As shown in Table 1, R_g ranged between 47 and 63 nm. For all the nano-objets (C_3^{DMSO}, C_3^{THF}, C_4^{DMSO}, and C_4^{THF}), the ratio R_g/R_h was estimated to be close to 1, which accounted for a vesicular morphology of the self-assemblies[38,39] and indicated that hollow spherical structures were obtained, whatever the initial nonselective solvent used (THF or DMSO).

To further investigate the morphology of the nanostructures, we have studied the dispersions of C3 and C4 by cryogenic transmission electronic microscopy (cryo-TEM). As shown in Figure 2a (case of C_3^{DMSO}), vesicles with a radius equal to 35 nm

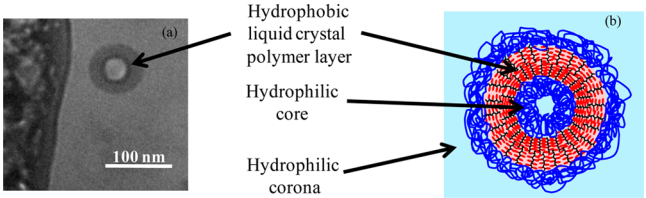

Figure 2. (a) Cryo-TEM image of polymersome obtained in water after dialysis of Dex-g^5-PADEGChol^{79} dispersed in THF (case of C_3^{THF}). (b) Schematic representation of such a vesicle.

(*z*-average) were actually observed. A schematic representation of such a vesicle is drawn in Figure 2b. The higher radius of vesicles found by DLS analysis compared to that estimated by cryo-TEM could be explained by hydration effects of the dextran corona that is extended in water. Moreover, dextran is less visible by cryo-TEM considering its swelling in water,

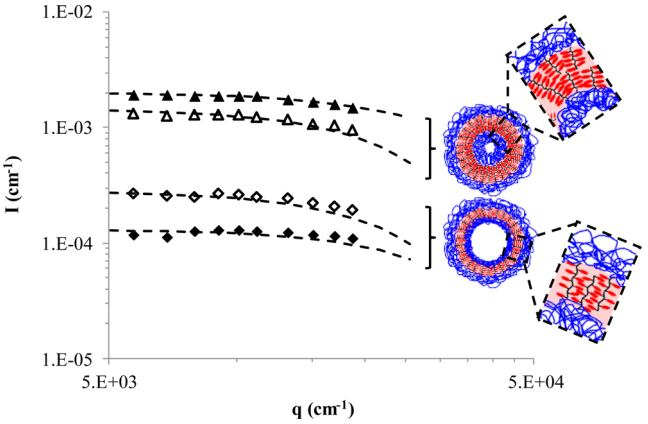

Figure 3. Scattered intensity (I) of vesicles as a function of scattering vector ($\mathbf{q}$) of (▲) C_3^{DMSO}, (Δ) C_3^{THF}, (◆) C_4^{DMSO}, and (◇) C_4^{THF}. Dashed lines are fits to eq S4. Schematic representations of vesicles and of their membranes are given.

leading to a low electronic contrast compared to water.[40] Supplementary images of the same nano-objects yet observed by TEM are presented in Supporting Information (Figure S4).

A more quantitative description of the self-assemblies has been achieved thanks to static light scattering measurements. Figure 3 displays the scattered intensity as a function of the scattering vector for each suspension (C_3^{DMSO}, C_3^{THF}, C_4^{DMSO}, and C_4^{THF}). The results could be fitted with a model developed for vesicles (eq S4).[41,42] We can then derive the thickness of the membrane (t) knowing the hydrodynamic radius of vesicle, the refractive index of aqueous medium (1.33), and that of the membrane made of PADEGChol (1.38), as reported in Table 1. A higher membrane thickness is obtained in the case of copolymer Dex-g^5-PADEGChol^{79}, which contains a higher number of grafts compared to that obtained for Dex-$g^{1.5}$-PADEGChol^{50}. That could be explained by the stiff nature of the PADEGChol grafts.[37] Actually, in the case of C_3^{DMSO} and C_3^{THF} suspensions, the polymeric membrane may consist of partially interdigitated grafts due to a higher grafting density onto the dextran backbone leading to steric hindrance. By opposition, in the case of C_4^{DMSO} and C_4^{THF}, the polymeric membrane may consist of fully interdigitated grafts, as shown in the schematic representation of Figure 3. The difference in the membrane thickness for C_4^{DMSO} and C_4^{THF} samples could be related to the better solubility of PDEGChol grafts in THF. Improved studies will be done in the future to confirm these observations.

After the synthesis of this first class of grafted glycopolymer containing liquid-crystal PDEGCholA grafts and a dextran backbone and the study of their mesomorphic properties, the ability of Dex-g^N-PDEGCholA^F to stabilize liquid−liquid interfaces were first proved. Then, self-assembly of such a glycopolymer was studied after dissolution in THF or DMSO and dialysis against water. Dynamic and static light scattering allowed the observation of spherical nanostructures (R_h between 47 and 68 nm, R_g/R_h close to 1), which are formed depending on the Dex-g^N-PDEGCholA^F structure. Finally, cryo-TEM observations clearly showed a hollow vesicular structure known as polymersome. Based on these results, a proper design of Dex-g^N-PDEGCholA^F led to polymersome formulations. It seems that a moderate number of long PDEGCholA grafts allows an adapted copolymer folding and a bilayer membrane formation, which is stabilized due to the

DOI: 10.1021/acsmacrolett.5b00471
ACS Macro Lett. 2015, 4, 1119−1122

liquid-crystal properties of PDEGCholA grafts. Deeper analyses of such Dex-g^{N}-PDEGCholA^{F} self-assemblies will be performed to gain a better understanding of the organic solvent influence and to investigate in-depth these vesicular morphologies. Nevertheless, such graft copolymers could have an interest for drug delivery systems: first, the materials involved in these copolymers (dextran and PDEGCholA) are biocompatible; second, the neutral dextran backbone may confer a stealthy character to nanostructures like PEGylation coverage;[43] and third, hydroxyl groups present on dextran could be used for functionalizing the surface of the nano-objects with a sufficient and consequent amount of "bioactive" molecules like specific peptides, for instance.[43]

■ ASSOCIATED CONTENT

Supporting Information

The Supporting Information is available free of charge on the ACS Publications website at DOI: 10.1021/acsmacrolett.5b00471.

Copolymer synthesis strategy, interfacial tension measurements, copolymer self-assembly procedure, dynamic and static light scattering (SLS and DLS), and transmission electronic microscopy (PDF).

■ AUTHOR INFORMATION

Corresponding Author

*E-mail: jean-luc.six@univ-lorraine.fr.

Notes

The authors declare no competing financial interest.

■ ACKNOWLEDGMENTS

K.F. was supported by a grant of the French Ministry in charge of Research.

■ REFERENCES

(1) Barenholz, Y. *Curr. Opin. Colloid Interface Sci.* **2001**, *6*, 66−77.
(2) Discher, B. M.; Won, Y.-Y.; Ege, D. S.; Lee, J. C.-M.; Bates, F. S.; Discher, D. E.; Hammer, D. A. *Science* **1999**, *284*, 1143−1146.
(3) Le Meins, J.-F.; Sandre, O.; Lecommandoux, S. *Eur. Phys. J. E: Soft Matter Biol. Phys.* **2011**, *34*, 1−17.
(4) Kumar, M.; Grzelakowski, M.; Zilles, J.; Clark, M.; Meier, W. *Proc. Natl. Acad. Sci. U. S. A.* **2007**, *104*, 20719−20724.
(5) Dao, T. P. T.; Fernandes, F.; Er-Rafik, M.; Salva, R.; Schmutz, M.; Brûlet, A.; Prieto, M.; Sandre, O.; Le Meins, J.-F. *ACS Macro Lett.* **2015**, *4*, 182−186.
(6) Onaca, O.; Enea, R.; Hughes, D. W.; Meier, W. *Macromol. Biosci.* **2009**, *9*, 129−139.
(7) Blanazs, A.; Armes, S. P.; Ryan, A. J. *Macromol. Rapid Commun.* **2009**, *30*, 267−277.
(8) Brinkhuis, R. P.; Rutjes, F. P. J. T.; Van Hest, J. C. M. *Polym. Chem.* **2011**, *2*, 1449−1462.
(9) Ohya, Y.; Takahashi, A.; Nagahama, K. *Adv. Polym. Sci.* **2011**, *247*, 65−114.
(10) Kita-Tokarczyk, K.; Grumelard, J.; Haefele, T.; Meier, W. *Polymer* **2005**, *46*, 3540−3563.
(11) Du, J.; O'Reilly, R. K. *Soft Matter* **2009**, *5*, 3544−3561.
(12) Jia, L.; Cao, A.; Lévy, D.; Xu, B.; Albouy, P. A.; Xing, X.; Bowick, M. J.; Li, M. H. *Soft Matter* **2009**, *5*, 3446−3451.
(13) Zhang, C.; Liu, D.; Zhou, B.; Deng, J.; Yang, W. *React. Funct. Polym.* **2012**, *72*, 832−838.
(14) Zhou, Y.; Kasi, R. M. *J. Polym. Sci., Part A: Polym. Chem.* **2008**, *46*, 6801−6809.
(15) Ahn, S. K.; Le, L. T. N.; Kasi, R. M. *J. Polym. Sci., Part A: Polym. Chem.* **2009**, *47*, 2690−2701.
(16) Xu, J. P.; Ji, J.; Chen, W. D.; Shen, J. C. *Macromol. Biosci.* **2005**, *5*, 164−171.
(17) Zhang, X.; Boissé, S.; Bui, C.; Albouy, P. A.; Brûlet, A.; Li, M. H.; Rieger, J.; Charleux, B. *Soft Matter* **2012**, *8*, 1130−1141.
(18) Jia, L.; Liu, M.; Di Cicco, A.; Albouy, P. A.; Brissault, B.; Penelle, J.; Boileau, S.; Barbier, V.; Li, M. H. *Langmuir* **2012**, *28*, 11215−11224.
(19) Zhou, Y.; Ahn, S.; Lakhman, R. K.; Gopinadhan, M.; Osuji, C. O.; Kasi, R. M. *Macromolecules* **2011**, *44*, 3924−3934.
(20) Mahmud, A.; Patel, S.; Molavi, O.; Choi, P.; Samuel, J.; Lavasanifar, A. *Biomacromolecules* **2009**, *10*, 471−478.
(21) Jia, L.; Albouy, P. A.; Di Cicco, A.; Cao, A.; Li, M. H. *Polymer* **2011**, *52*, 2565−2575.
(22) Pinol, R.; Jia, L.; Gubellini, F.; Levy, D.; Albouy, P. A.; Keller, P.; Cao, A.; Li, M. H. *Macromolecules* **2007**, *40*, 5625−5627.
(23) Liu, C. L.; Lin, C. H.; Kuo, C. C.; Lin, S. T.; Chen, W. C. *Prog. Polym. Sci.* **2011**, *36*, 603−637.
(24) Li, M. H.; Keller, P. *Soft Matter* **2009**, *5*, 927−937.
(25) Meng, F.; Zhong, Z.; Feijen, J. *Biomacromolecules* **2009**, *10*, 197−209.
(26) Soliman, S. M. A.; Nouvel, C.; Babin, J.; Six, J. L. *J. Polym. Sci., Part A: Polym. Chem.* **2014**, *52*, 2192−2201.
(27) Popescu, M. T.; Tsitsilianis, C. *ACS Macro Lett.* **2013**, *2*, 222−225.
(28) Olsen, D. B.; Segalman, R. A. *Mater. Sci. Eng., R* **2008**, *62*, 37−66.
(29) Klok, H. A.; Lecommandoux, S. *Adv. Mater.* **2001**, *13*, 1217−1229.
(30) Schatz, C.; Lecommandoux, S. *Macromol. Rapid Commun.* **2010**, *31*, 1664−1684.
(31) Carlsen, A.; Lecommandoux, S. *Curr. Opin. Colloid Interface Sci.* **2009**, *14*, 329−339.
(32) Popescu, M. T.; Korogiannaki, M.; Marikou, K.; Tsitsilianis, C. *Polymer* **2014**, *55*, 2943−2951.
(33) Lee, H. J.; Yang, S. R.; An, E. J.; Kim, J.-D. *Macromolecules* **2006**, *39*, 4938−4940.
(34) Kim, M. S.; Lee, D. S. *Chem. Commun.* **2010**, *46*, 4481−4483.
(35) Gao, K. J.; Liu, X. Z.; Li, G.; Xu, B. Q.; Yi, J. *RSC Adv.* **2014**, *4*, 59323−59330.
(36) Babinot, J.; Guigner, J.-M.; Renard, E.; Langlois, V. *Chem. Commun.* **2012**, *48*, 5364−5366.
(37) Ferji, K.; Nouvel, C.; Babin, J.; Albouy, P. A.; Li, M. H.; Six, J. L. *J. Polym. Sci., Part A: Polym. Chem.* **2013**, *51*, 3829−3839.
(38) Stauch, O.; Schubert, R.; Savin, G.; Burchard, W. *Biomacromolecules* **2002**, *3*, 565−578.
(39) Houga, C.; Giermanska, J.; Lecommandoux, S.; Borsali, R.; Taton, D.; Gnanou, Y.; Le Meins, J. F. *Biomacromolecules* **2009**, *10*, 32−40.
(40) Filippov, S. K.; Lezov, A. V.; Sergeeva, O. Y.; Olifirenko, A. S.; Lesnichin, S. B.; Domnina, N. S.; Komarova, E. A.; Almgren, M.; Karlsson, G.; Štepanek, P. *Eur. Polym. J.* **2008**, *44*, 3361−3369.
(41) Hallett, F. R.; Watton, J.; Krygsman, P. *Biophys. J.* **1991**, *59*, 357−362.
(42) Jaskiewicz, K.; Larsen, A.; Schaeffel, D.; Koynov, K.; Lieberwirth, I.; Fytas, G.; Landfester, K.; Kroeger, A. *ACS Nano* **2012**, *6*, 7254−7262.
(43) Bertholon, I.; Vauthier, C.; Labarre, D. *Pharm. Res.* **2006**, *23*, 1313−1323.

DOI: 10.1021/acsmacrolett.5b00471
ACS Macro Lett. 2015, 4, 1119−1122